# Percussion Nd:YAG Laser-incision of Radiata Pine: Effects of Laser Processing Parameters and Wood Anatomy

Nath, Subhasisa; Waugh, David; Ormondroyd, Graham; Spear, Morwenna; Curling, Simon; Pitman , Andrew ; Mason , Paul

**Lasers in Manufacturing and Materials Processing**

*DOI:*
https://doi.org/10.1007/s40516-022-00169-3

Published: 01/06/2022

Peer reviewed version

# Percussion Nd:YAG laser-incision of Radiata Pine: Effects of laser processing parameters and wood anatomy

Subhasisa Nath[1], David Waugh[1], Graham Ormondroyd[2], Morwenna Spear[2], Simon Curling[2], Andy Pitman[3], Paul Mason[4]

[1]**School of Mechanical, Automotive and Aerospace Engineering, Coventry University, Gulson Road, Coventry, CV1 2JH, UK.*
[2]*The Biocomposites Centre, Bangor University, Bangor, LL57 2UW, UK.*
[3]*LIGNIA Wood Company Limited, Unit 10, Atlantic Trading Estate, Barry, CF63 3RF, UK.*
[4]*Millennium Lasers Limited, Units 3-5, Llan Coed Court, Coed Darcy, Llandarcy, Neath, SA10 6FG, UK.*

**Corresponding author:* sendsubha@gmail.com

**Abstract**

Laser-incision is gaining recognition in the timber processing industry as a preferred and competitive technique for increasing uptake of chemical and preservative treatments. This work details percussion Nd:YAG laser-incision of Radiata Pine, conducted at different wavelengths, incident laser energies and focal point positions. For the first time, the effect of wood anatomy (latewood and earlywood tissues) on the efficiency and quality of Nd:YAG laser-incision of Radiata Pine is explored. Nd:YAG laser wavelengths of 1064 nm (fundamental wavelength), 532 nm (second harmonic) and 355 nm (third harmonic) were used to understand their effect on laser-incised hole characteristics. A maximum laser-incised hole diameter of ~ 2.5 mm was measured at 1064 nm for 700 pulses. The presence of earlywood and latewood had a distinct effect on hole shape evolution, showing the importance of wood anatomy in the process of percussion Nd:YAG laser-incision. Ultra-violet (UV) radiation (355nm) was the preferred wavelength for laser-incision of Radiata Pine as it gave rise to less carbonisation, less tapering and a uniform incision along the length of the laser-incised holes. Maximum depth of the laser-incised hole was measured (~ 20 mm) using the 355 nm wavelength. Incident laser energy, wavelength and wood anatomy had a dominant role in laser-incision hole size, shape and quality. This demonstrates the critical effect of wood anatomy on the laser-incision process when considering and utilising laser technology to produce incisions for the wood treatment and wood preservation industries.

*Keywords*: Laser-incision; Nd: YAG laser; Wood; Hole; Microstructure

## 1. Introduction

Timber is a natural material and has been used in construction for many millennia and is one of the most sustainable and environmentally favourable materials. Timber is also a suitable alternative to other structural materials due to its high strength-to-weight ratio and reduced energy requirements in manufacture [1–4]. Timber is usually classified as either hardwood, from broadleaved trees, such as beech and oak, or softwood from conifers, like pine and fir. Because they are renewable, fast-growing plantation softwoods tend to be sustainable, when well-managed. However, the constituent polymers of wood (cellulose, hemicellulose and lignin) are not resistant to weather, insect or fungal attack particularly when the moisture content exceeds 20% in service. Chemical (preservative) treatments are widely used to protect the wood polymers against degradation and overall failure of timber components [5,6]. More recently, other technologies such as wood modification have been developed which avoid the use of biocides, but provide protective effects through physical or chemical changes in the wood [7]. The effectiveness of preservative treatments and some wood modification techniques depend on a suitable depth of penetration of chemicals into the wood structure. This is influenced by permeability characteristics of the wood species [8,9]. Interventions such as mechanical incising are known to improve permeability, and new strategies or improved methods are required to achieve higher levels of performance.

The structure of wood influences the permeability. The permeability is improved when the longitudinal and transverse flows of impregnated chemicals is achieved which isn't seen in every wood species. Conventional methods for treating wood, using vacuum and pressure, are known to have limited effect in impregnation of some woods such as spruce, due to the aspiration of bordered pits which connect adjacent wood cells [8,10,11]. Researchers have attempted to improve permeability using steam pre-treatments, microwave treatments, ultrasonic treatments, bio-incising, mechanical incising and laser incising. Several pre-treatment methods have been shown to increase the preservative retention in the wood [5]. Of these, incising has proven beneficial in increasing the penetration and retention of chemical preservatives [12,13], with laser-incising being increasingly preferred, due to its ability to incise deeper, use smaller hole dimensions and the laser being a non-contact method, with lower wear on tooling [12,14]. Laser-incised deep holes help the preservative chemicals to reach deeper and distribute along

the longitudinal and transverse flow paths in the wood structure. Several thousands closely spaced holes are needed to improve the overall permeability dependent on the wood species.

A laser provides flexibility, precision, and reproducibility in drilling quality holes of any desired shape and size into metals, ceramics, polymers, and composites regardless of the physical and mechanical properties of the material [15–18]. Lasers have been used mostly for marking, engraving and cutting of woods [19–21]. The wavelength of a laser has a strong influence on the machining (including incising) characteristics of wood [14,22–25]. With wavelengths in the near-infrared (NIR) range, poor or no machining of wood has been observed in previous studies, due to poor absorption of the laser radiation by the wood [14], although little consideration of wood anatomy was given study. Laser radiation in the ultra-violet (UV) and the far-infrared (FIR) regions were well absorbed (> 80%) by most wood species and thus are preferred wavelengths for wood, giving optimal material processing [26]. $CO_2$ lasers with radiation in the FIR regime have been previously used for laser-incision of woods due to their ability to attain the higher power density necessary to speed up processing [25–34]. It emerged that wood anatomy can play a role in incision efficiency, influencing hole depth, diameter and circularity. Nath *et al.* [27] recently reported that the presence of earlywood and latewood had a significant influence on the incision properties during $CO_2$ laser incising. Laser interactions with the denser latewood tissues resulted in shallower holes.

Longer laser pulse durations during laser-incising led to structural degradation due to the formation of the heat-affected zone (HAZ), charring and carbonisation [26,28–32]. The use of high powers during laser processing of wood resulted in its melting and formation of wood charcoal on the surface [35]. Lignin decomposition and deposition of substances were reported following $CO_2$ laser-incision of wood, as lignin decomposes at temperatures between 280–550 °C [28]. The peak rise in temperature during $CO_2$ laser cutting of wood was reported to be 4750°C [24]. Longer pulse durations in the range of 50 ms to 300 ms have been found to produce significant HAZ in the laser-incised woods due to increased heat diffusion lengths [28]. Better control of the HAZ can be achieved with a shorter pulse duration due to the reduction of the heat diffusion length during laser-wood interaction [29]. The heat flow to the surrounding wood areas during UV (355 nm) laser machining was reported to be less, owing to the rate of heating and the rate of evaporation being instantaneous. This process was based on ablation only

[14,36]. On the other hand, with wavelengths of 532 nm and 1064 nm, the rate of heating was slower, resulting in increased heat flow to the surrounding areas. This gave rise to increased carbonisation during laser machining of the wood [14]. Moreover, UV lasers have been beneficial for producing high aspect ratio holes during laser drilling with significantly less charring [14,36]. Less structural damage to the wood was also reported with an excimer laser than $CO_2$ laser [26].

Most studies to date have focussed on $CO_2$ laser-incising of wood because of faster processing speeds offered, but at the cost of structural degradation of wood. Although there has been little discussion of the influence of structural degradation on preservative flow, some believe the holes permit additional access to the interior of the timber for bulk flow whereas others reported that structural changes such as formation of HAZ alter wettability of the wood surface at the incision, negatively affecting preservative flow although this is outweighed by bulk flow [28]. Less work has been done on UV laser-incision of woods to produce deep holes [14,23,26,36,37]. In the present study, the relationships between the laser wavelength, its fluence, and focal point position on the incision efficiency, shape, size and quality of incised holes have been established. A critical analysis of the laser-incision process has been undertaken to report on the mechanism and factors affecting the laser-incision process, and establish importance of the wood anatomy on percussion laser-incision.

## 2. Experimental Technique

### *2.1. Materials*

In the present study, Radiata Pine was used for the laser-incision. The blocks were machined to 100 mm × 35 mm × 30 mm from a single piece and had a fine sawn finish. Table 1 presents the air-dry density and the moisture content at time of incisingdetermined according to BS EN 13183-1:2002.

**Table 1** Moisture content (%) and density of Radiata Pine used in the present study.

| Species | Moisture content (%) | Density ($kg/m^3$) |
|---|---|---|
| Radiata Pine | 7.92 | 400 |

### *2.2. Laser-incision experiments*

Laser-incision was carried out using a pulsed Nd:YAG laser (Q-Smart 850, Quantel, UK). The fundamental wavelength of the laser was 1064 nm. Second and third harmonic modules were attached to

operate the laser in 532 nm (2ω) and 355 nm (3ω) regimes. The laser pulse energy at 1064 nm, 532 nm and 355 nm was measured by placing the power meter after the focusing lens away from the focal plane. The desired pulse energy was achieved by adjusting the Q-switch delay. The energy stability was ± 2% and the beam divergence was < 0.5 mrad. The focusability ($M^2$) of the laser beam at 1064 nm was ≤ 2. The theoretical focal spot size was calculated using the theoretical focussing diameter ($d_0$) equation given in Equation (1).

$$d_0 = \frac{4 \cdot \lambda \cdot f \cdot M^2}{\pi \cdot D_{raw}} \qquad (1)$$

With a raw laser beam diameter ($D_{raw}$) of 9 mm and, using a fused silica lens, a focal length ($f$) of 135 mm Equation (1) gave a theoretical focal spot size for each wavelength ($\lambda$) of 41 µm (at $\lambda$ = 1064 nm), 20 µm (at $\lambda$ = 532 nm) and 14 µm (at $\lambda$ = 355 nm).

The peak laser fluence ($F$) on the surface of the workpiece was calculated by the equation presented in Equation (2).

$$F = \frac{2E_P}{\pi r_0^2} \qquad (2)$$

where $E_P$ is the laser pulse energy and $r_0$ is the focal spot size.

The laser-incisions were conducted on the radial faces of the wood samples. Five holes were laser-incised for each parameter combination (laser wavelength, pulse energy and number of pulses) on each wood block. Woodblocks used were selected at randomly from the set processed. A percussion mode was used for the laser-incision study, with the number of laser pulses ranging from 100 to 700. The process parameters adopted in the present study are set out in Table 2.

**Table 2** Laser-incision parameters used in the present study.

| Parameters | Nd: YAG laser | | |
|---|---|---|---|
| Wavelength | 1064 nm | 532 nm | 355 nm |
| Pulse energy | 320 mJ and 850 mJ | 320 mJ and 450 mJ | 7 mJ, 25 mJ, 50 mJ, 100 mJ, 150 mJ, 200 mJ, 250 mJ, 320 mJ |
| Theoretical focal spot size | 41 µm | 20 µm | 14 µm |
| Mode | Pulsed | | |
| Technique | Percussion | | |

| | |
|---|---|
| Pulse duration | 6 ns |
| Repetition rate | 10 Hz |
| Energy stability | ± 2% |
| Focusability ($M^2$) | ≤ 2 @ 1064 nm |
| Beam divergence | < 0.5 mrad |

*2.3. Hole shape and size analysis*

Following percussion laser-incision, optical microscopy (Leica S6 D Stereozoom; Leica Mycrosystems AG, Switzerland) was used to measure the hole diameter on the surface and hole depth following sectioning through the wood specimen. To measure the depth of laser-incised holes, a sander was used to expose the hole, following which a compressed air jet was used to remove any sanding residue. Prior to microstructural analysis, the wood samples were oven-dried for 2 hours at 50 °C to remove moisture then sputter-coated with gold-palladium mixture for 180 seconds. The laser-incised hole structure was examined using a field emission scanning electron microscope (Gemini FESEM; ZEISS). The electron beam acceleration voltage and the beam-specimen working distance were adjusted to 20 kV and ~6 mm, respectively.

## 3. Results and Discussion

*3.1. Microscopic analysis of laser-incised woods*

Fig. 1 shows the optical micrographs of the top surface of Nd: YAG laser-incised holes in Radiata Pine for different laser wavelengths, incident laser energies and number of laser pulses. It is evident from Fig. 1 that the laser-incised holes were near circular for all wavelengths except 355 nm which gave rise to an asymmetrical holes. The asymmetrical holes at 355 nm were due to higher material removal rate causing hole edge disturbance. From Fig. 1, it can be observed that the hole surface and wall became darker which implies increased charring and carbonisation. Due to lower absorption of laser radiation (lower absorbed laser intensity) by the wood at 1064 nm, the material removal rate was lower and the absorbed intensity was not enough to cause increased laser ablation.

The energy absorbed by the wood was mostly used to heat the material which caused significant charring and carbonisation on the surface of the laser-incised holes and its wall. The severity of charring and carbonisation was higher at a higher incident pulse energy and wavelength. With the increase in

absorption of laser radiation by the wood at shorter wavelengths (532 nm and 355 nm), the ablation rate (or the material removal rate) increased resulting in less charring and carbonisation at the hole surface. The laser-incised hole at 355 nm shows significantly less carbonisation due to greater absorption of laser radiation as compared to 1064 nm and 532 nm wavelengths. The laser pulse number also had a significant effect on carbonisation, with increasing pulse number increasing carbonisation.

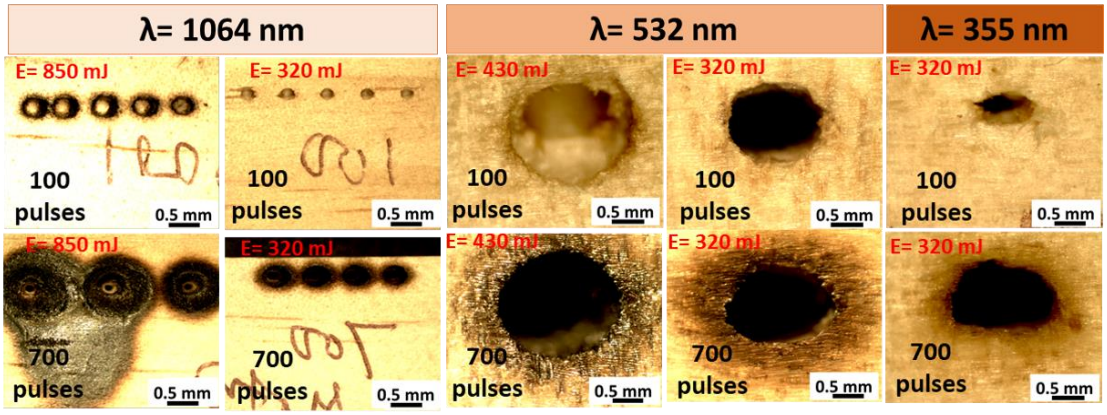


**Fig. 1** Optical micrographs showing the top view of Nd: YAG laser-incised holes in Radiata Pine for different wavelengths, incident laser energies and laser pulses (top layer of micrographs shows laser pulse number of 100 and bottom layer shows the laser pulse number of 700).

Fig. 2 shows the optical micrographs of the cross-section of Nd: YAG laser-incised holes in Radiata Pine for different wavelengths, incident laser energies and number of laser pulses. It is apparent that the charring and carbonisation were greatest and mostly located in the upper hole for 1064 nm wavelength.. A wider heat affected zone (HAZ) can be seen around incisions formed using 1064 nm wavelength as compared to 532 nm and 355 nm laser wavelengths. Poor absorption of laser radiation at 1064 nm was responsible for increased charring and carbonisation. Hole taper was more evident at 1064 nm than at shorter wavelengths. The degree of charring was also higher at higher incident laser energies. At a wavelength of 355 nm, the holes showed less charring, carbonisation and more uniform hole depth (i.e. less taper). By selecting shorter wavelength hole size is reduced along with charring and carbonisation which have a negative impact on appearance

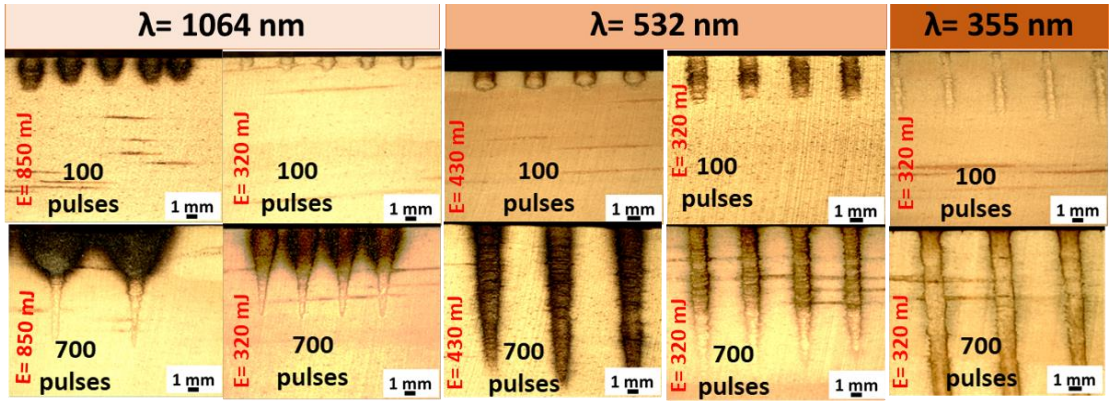


**Fig. 2** Optical micrographs showing a cross-sectional view of laser-incised holes in Radiata Pine Pine for different wavelengths, incident laser energies and laser pulses (top layer of micrographs shows laser pulse number of 100 and bottom layer shows the laser pulse number of 700).

*3.2. Effect of wood anatomy on the characteristics of laser-incised holes*

Fig. 3 shows the difference in the shapes of laser-incised holes on the radial face of Radiata Pine. Both were incised with a laser wavelength of 355 nm and laser fluence of $4.16 \times 10^3$ J/mm$^2$ for 700 laser pulses. Fig. 3 (a) shows the laser-incision into the latewood tissue while Fig. 3 (b) shows laser-incision of the growth ring interface, straddling the earlywood and latewood. The measured laser-incision hole diameters for samples in Fig. 3 (a) and Fig. 3 (b) were 0.59 mm and 1.1 mm, respectively. The laser-incised hole was not symmetrical considering a gaussian laser beam was used. From Fig. 3 (b) the laser interaction with the earlywood and latewood tissues resulted in larger and smaller hole diameters, respectively. Thus, laser-incision rate was affected by density, with greater removal of lower density earlywood than higher density latewood. Other studies reported lower incision rates in denser woods and differences, as shown in between earlywood and latewood. The denser latewood resulted in an asymmetrical hole as denser wood absorbs greater laser radiation.

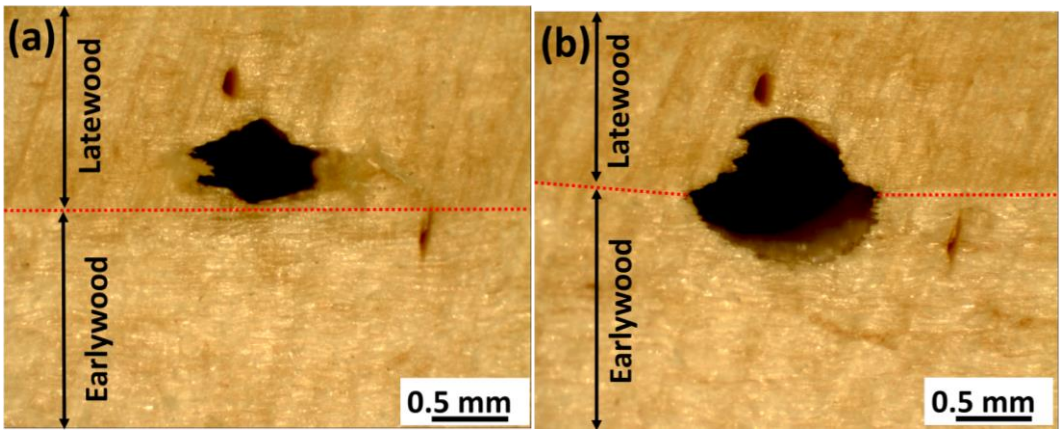

**Fig. 3** Optical micrographs showing the difference in the shape of laser-incised holes on the radial face of Radiata Pine, both incised with a laser wavelength of 355 nm and laser fluence of $4.16 \times 10^3$ J/mm$^2$ for 700 laser pulses ((a) shows the laser-incision into the latewood tissue and (b) shows laser-incision of the growth ring interface, straddling the earlywood and latewood).

Different scenarios for the interaction of a laser beam with earlywood and latewood tissues are depicted in Fig. 4, based on the growth ring alignment within the wood, and indicating likely incision depths resulting from typical orientations and interaction with earlywood and latewood tissues. The dimensions and ratios of the earlywood and latewood tissues within the growth rings varies with wood species, growing conditions and wood age. The density of Radiata Pine latewood was reported to be 1.4 to 1.6 times higher than earlywood [38]. When laser-incising the radial face, the interaction of a laser beam with earlywood tissue (Fig. 4 (a)) resulted in a higher diameter and greater depth hole. On the other hand, laser beam interaction with the latewood tissue (Fig. 4 (b)) resulted in smaller diameter and shallower hole. If the timber is oriented to present the tangential face for laser-incision, the laser beam interaction with the wood tissues differs, depending on the number of growth rings per centimetre, and latewood:earlywood ratio. The ratio of latewood to earlywood was reported to vary from 0.09 to 0.15 in juvenile wood and 0.17 to 0.32 in mature wood [39] and this will impact depth and diameter of incisions across these wood types. Another possible orientation of earlywood and latewood tissues is the earlywood and latewood tissues may be oriented at an angle (this example shows around 45°) to the incident laser beam. Therefore, the presence, shape, dimensions and orientation of earlywood and latewood tissues will contribute to the final hole diameter and depth. This is of considerable importance when establishing the settings for laser-incising timber in an industrial process, to ensure sufficient incision depth for pieces, regardless of growth ring orientation. All growth ring arrangements may be found in pieces when logs are processed into pieces.

When moving from laboratory tests to industrial systems this highlights the importance of taking the anticipated range of earlywood/latewood ratios, piece densities and timber-laser interactions into consideration. This is in accordance with previous work for $CO_2$ laser-incision of woods [27].

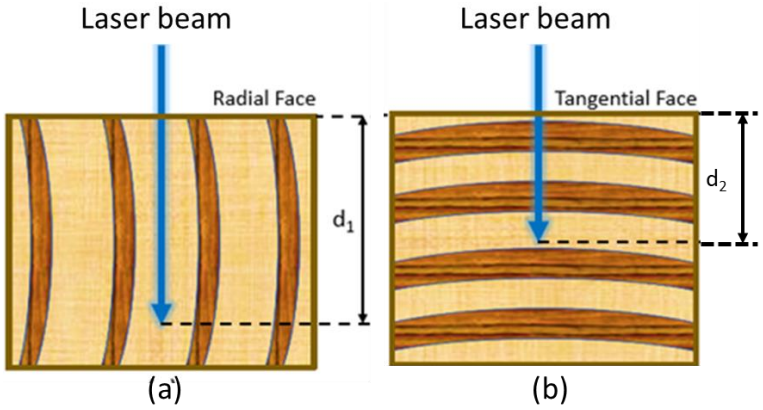


**Fig. 4** Schematic representation of the effect of wood structure on laser-incision. (a) laser-incision into earlywood region through radial face and (b) laser-incision into tangential face passes through both earlywood and latewood.

Fig. 5 shows the scanning electron micrographs of pulsed Nd: YAG laser-incised regions in Radiata Pine with an incident laser energy of 320 mJ for 100 pulses with wavelengths of (a, d) 1064 nm, (b, e) 532 nm and (c, f) 355 nm. The extent of material removal in the laser-incision process depends on laser wavelength, with higher laser wavelengths causing less material removal, corresponding with the lower incision rate reported earlier. Light microscopy of the laser-incised structure (i.e. hole wall) also revealed that there was increased carbonisation with the increase in the laser wavelength (Fig. 2), while SEM revealed that with the 1064 nm wavelength the tracheids had been separated, leading to a 'fibrous appearance' as if middle lamella had been preferentially removed (Fig. 5 (a,d)), whereas the shorter wavelengths led to complete removal of the cell wall (Fig. 5 (e,f)). The increased laser-incision rate and removal of cell wall materials by a decomposition, vapourisation and plasma formation have acted more efficiently at decreased laser wavelength, this is related to the increased absorption of laser radiation by the wood in the UV region. Higher photon energy at a smaller wavelength also contributed to the increased depth of holes and increased structural modification.

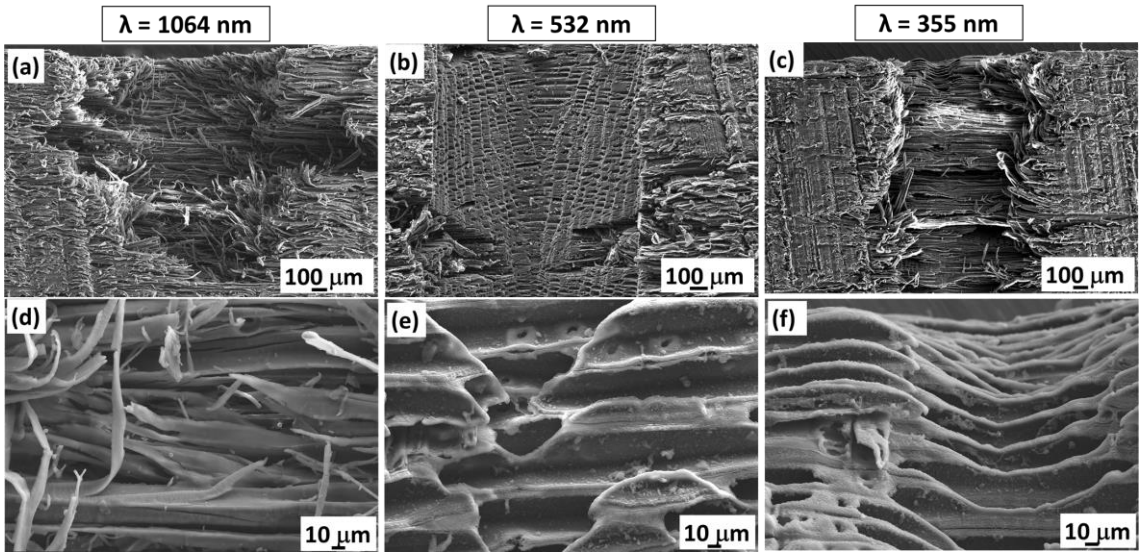


**Fig. 5** Scanning electron micrographs of the cross-section of Nd: YAG laser-incised holes in Radiata Pine at an incident laser energy of 320 mJ incised for 100 pulses with wavelengths of (a, d) 1064 nm, (b, e) 532 nm and (c, f) 355 nm.

Fig. 6 shows the scanning electron micrographs of the cross-sections of Nd: YAG laser-incised holes in Radiata Pine with a laser wavelength of 355 nm for (a, c) 100 pulses and (b, d) 700 pulses. Fig. 6 confirms the deposition of carbonaceous products from the aerosol or vapour state, on the laser-incised hole wall. Both UV and IR radiations have been reported to be responsible for decomposition and carbonisation of cellulose following laser ablation [26]. The observed deposition of carbonised and aerosol material on the wood structure were found to be uniform throughout the laser-incised hole for 355 nm wavelength. Thermal decomposition of wood cell wall polymers is known to occur at 200–260 °C for hemicelluloses, 230–340 °C for cellulose and 290–500 °C lignin [29]. The deposition of carbonaceous products was observed above 100 laser pulses in the Nd: YAG laser-incision, which indicates that process temperature during Nd: YAG laser incising exceeded the thermal decomposition temperature of wood polymers. This phenomenon is widely recognised, for example Panzer *et al.* [26] reported the melting and deposition of foam-like products for both UV and infrared wavelengths. Naderi *et al.* [40] also reported similar wood structure modification during laser processing of wood. Use of inert gas during laser cutting of wood has been reported to reduce charring and deposition of carbonaceous products [41]. Deposition of the carbonaceous products was reported to be laser-induced graphene (LIG) [42–44]. Wood samples with higher lignin contents were reported to be easily carbonised and formed LIG [43]. LIG forms at low laser powers (1.6 to 8.6 W) and with shorter pulse durations under an inert atmosphere [42,44]. In the present study, no inert atmosphere was used. Whilst it is believed that LIG has been formed, further tests are

necessary to confirm this and to investigate its effects on fluid flow from holes into adjacent wood tissues with preservative treatment.

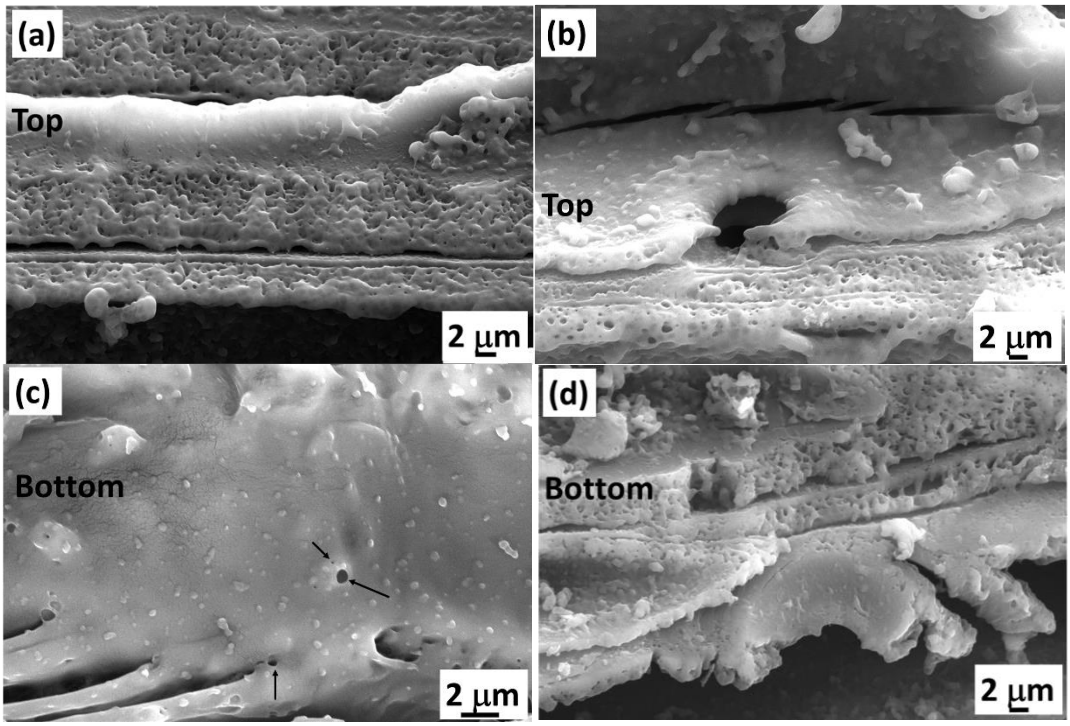


**Fig. 6** Scanning electron micrographs of the cross-section of Nd: YAG laser-incised holes in Radiata Pine with a laser wavelength of 355 nm for (a, c) 100 pulses and (b, d) 700 pulses.

*3.3. Effect of laser wavelength on the diameter of the incised hole*

Fig. 7 shows the effects of Nd: YAG laser wavelength on the diameter of laser-incised holes at a constant laser energy of 320 mJ. The largest laser-incised hole diameter of ~2.5 mm was measured for the sample incised with the 1064 nm wavelength, with 700 pulses. This was due to the larger laser beam diameter, at focus, when operating at 1064 nm. The focussed Nd:YAG laser beam diameters at 1064 nm, 532 nm and 355 nm were calculated to be 41 μm, 20 μm and 14 μm, respectively. When influence of laser wavelength on hole diameter were compared in conjunction with pulse number the 1064 nm wavelength only resulted in largest diameter holes when the number of pulses were greater than 300. On the other hand, with laser pulse numbers between 100 and 300 pulses, a maximum diameter was measured at the 532 nm wavelength. Laser-incised holes at 355 nm had lowest diameters for most laser pulse numbers. It was expected that the diameter of holes would correlate with the focussed beam diameters at 1064 nm (~41 μm), 532 nm (~20 μm) and 355 nm (~14 μm).

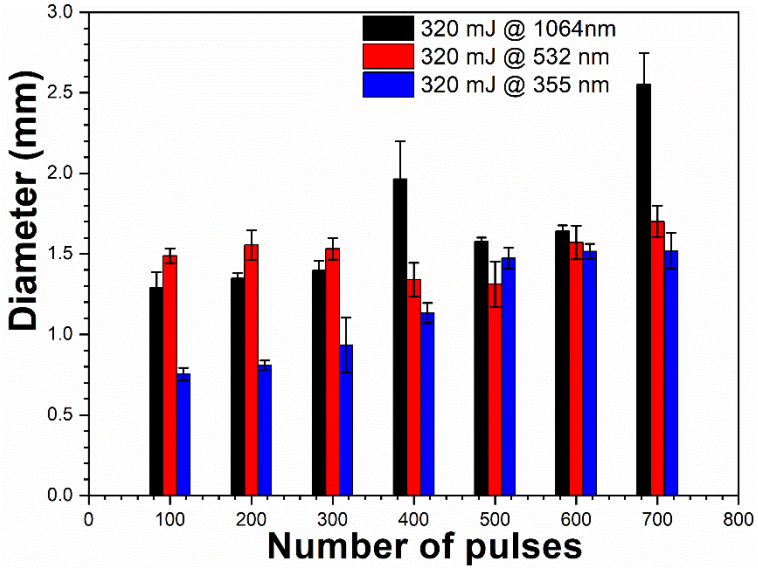


**Fig. 7** Variation of laser-incised hole diameter with varying laser wavelength in Radiata Pine.

From Fig. 7 for laser pulses between 400 and 700 the relationship between wavelength and hole diameter holds true However, the measured hole diameters at 1064 nm and 532 nm for 500 pulses, and 300 pulses and lower did not support the hypothesis that incised hole diameter relates tolaser beam diameter at the surface shown in Fig. 8 (a). Considering the mechanism of laser-incision, as depicted in Fig. 8 (b), the material removal occurred by (1) classical laser energy absorption, (2) heating of the material, (3) decomposition, (4) evaporation, (5) plasma formation, and (6) outward vapour ejection due to recoil pressure. The ejection of vaporised material away from the hole front is responsible for the laser-incised hole shape (taper) and size (diameter and depth) as the ejected materials will erode the hole wall as laser irradiation continues. The near-surface hole wall is therefore eroded over a longer period giving rise to an increase in the entry-hole diameter as compared to the bottom of the hole. The absorption of laser radiation by wood was greatest at a wavelength of 355 nm and a minimum at 1064 nm [26]. Since absorption of the laser radiation at 1064 nm was lower than 532 nm wavelength, it explains why the latter resulted in larger diameter holes as shown in Fig. 7, for laser pulses less than 300 . However, the same hypothesis was not valid for laser pulses between 400 and 700 where laser beam size at focus had greater influence according to Fig. 8 (a). The smaller hole diameter at 1064 nm between 100 to 300 laser pulses, in Fig. 7 may also be a result of anatomical differences in specimens incised , as previously reported by Nath *et al* [27]. Radiata pine consists of alternating layers of earlywood and latewood, with denser latewood tissues less easily ablated [14,27,36]. One possible reason for smaller diameter holes at 1064 nm at lower pulse numbers could be that dense latewood was located on the surface of the wood leading

to less erosion. The other probable reason was the number of latewood tissues through the thickness of the wood block present in the laser-wood interaction zone. A dense structure absorbs more incident energy and attenuates the beam energy resulting in less material removal and erosion of entry hole wall.

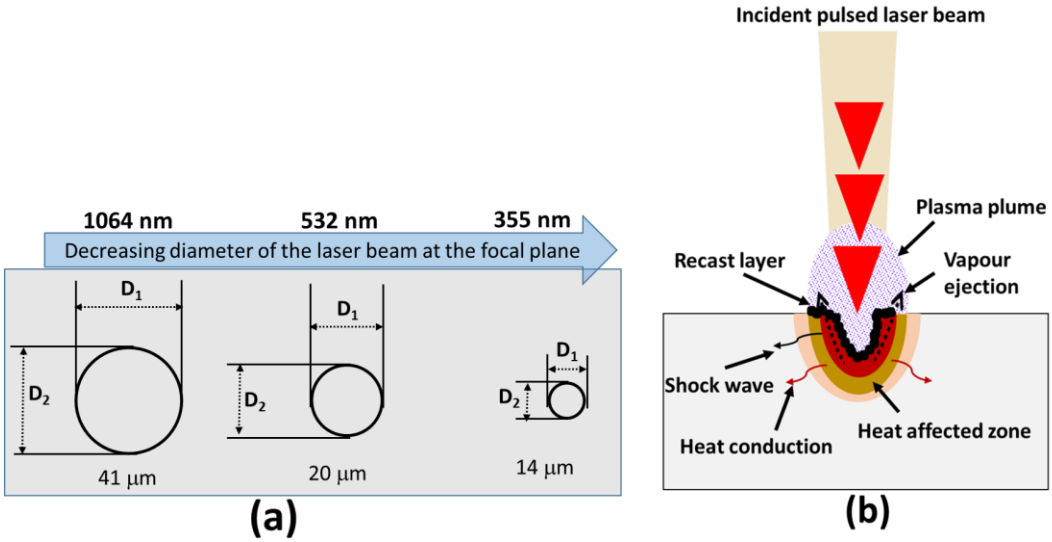


**Fig. 8** (a) Schematic representation of laser spot size with the laser wavelength, (b) laser-wood interaction mapping [45].

*3.4. Effect of laser wavelength on the depth of the incised hole*

The absorption of laser energy by wood depends on (a) optical charactristics of the wood, (b) wavelength of laser radiation and (c) laser energy density. Most of the organic polymers are transparent to the visible and near infrared radiations. Fig. 9 shows the effect of differing Nd: YAG laser wavelengths on the depth of incised holes. From Fig. 9, it is evident that the depth of hole increased by decreasing the wavelength from NIR (1064 nm) to UV (355 nm).. The maximum depth of laser-incised holes were around 20 mm for 355 nm wavelength. Comparing depth using the 1064 nm, 532 nm and 355 nm wavelengths, with a constant incident laser energy of 320 mJ, the depths of holes at 355 nm wavelength were 3 times greater than those at 1064 nmand at 532 nm nearly double..

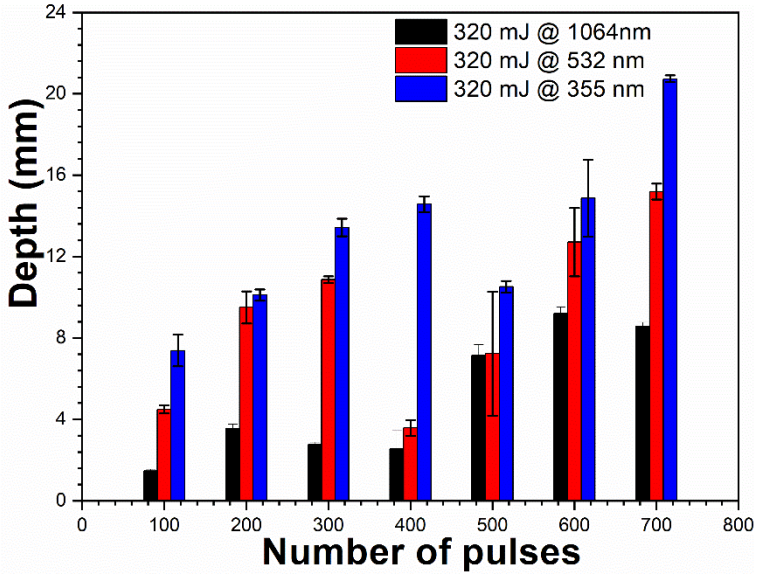


**Fig. 9** Variation of laser-incised hole depth with laser wavelength in Radiata Pine.

*3.5. Effect of incident laser energy on the diameter of the laser-incised hole*

Fig. 10 shows the variation of hole diameters with number of laser pulses for different incident laser energies at (a) 1064 nm and (b) 532 nm wavelengths. An increase in the incident laser energy increased the diameter of laser-incised holes irrespective of the laser wavelength, as shown in Fig. 10. A maximum diameter of approximately 6 mm was measured for the incident laser energy of 850 mJ at 1064 nm wavelength. From Fig. 10 (a), it should be noted that the diameter of the laser-incised hole, with an incident laser energy of 850 mJ at 1064 nm, was two to three times larger than the diameter measured following an incident laser energy of 320 mJ . Similarly, the diameter of the laser-incised hole at 532 nm with an incident laser energy of 450 mJ was higher than at 320 mJ except for 200 laser pulses and 300 laser pulses, as shown in Fig. 10 (b). The diameters of the incised holes at 200 laser pulses and 300 laser pulses were similar for 450 mJ and 320 mJ. This result was unexpected as an increase in incident laser energy would be expected to increase heat input and material removal. As incident laser energy was the only variable, it can be concluded that differences in wood anatomy was responsible for the observed behaviour for 200 and 300 laser pulses, with variations arising since holes were into either latewood or earlywood [27]. The laser beam diameter on the surface of the samples was measured to be 41 μm for 1064 nm laser wavelengths. However, measured laser-incised hole diameters at 1064 nm were 2.3 mm and 6.1 mm for 100 and 700 pulses at an incident laser energy of 850 mJ. The laser-incised hole diameter was not only greater than the laser beam diameter but also increased with the number of incident laser pulses. The laser-wood interaction can be considered according to Fig. 8 (b). In the beginning, the laser

energy was absorbed by the wood by the classical mechanism and material removal began by decomposition and vaporisation and subsequent ejection of vapour species out of the hole due to recoil pressure. As the number of pulses increased the vaporised material turned into a plasma cloud which expands with pulse number. A pressure gradient was created between the hole front and hole surface which drives vaporised material out of the hole bottom. The pressure gradient increased with an increase in the number of laser pulses and laser energy. The explosive ejection of the vaporised materials erodes the hole walls, causing the hole diameter to increase. Hole wall erosion was maximum near the surface of the hole and minimum at the hole bottom.

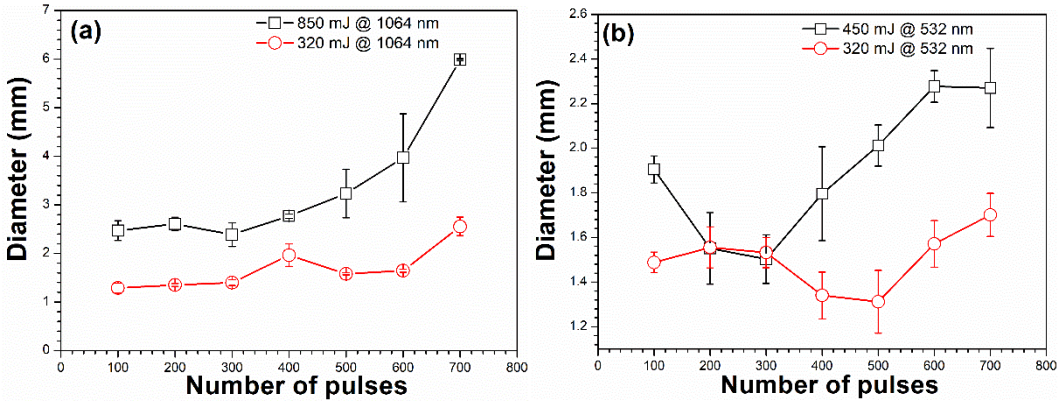


**Fig. 10** Variation of laser-incised entrance-hole diameter with laser energy at (a) 1064 nm and (b) 532 nm wavelengths in Radiata Pine.

*3.6. Effect of incident laser energy on the depth of the laser-incised hole*

Fig. 11 shows the variation in depth of the laser-incised holes with number of laser pulses for different incident laser energies at (a) 1064 nm and (b) 532 nm laser wavelengths. Overall, the depths of the holes increased with the number of laser pulses for all incident laser energies Fig. 11 (a) and Fig. 11 (b). In a small number of cases an increased number of pulses did not result in greater hole depth which is likely to result from anatomical differences between wood specimens used. Material removal increased with the number of laser pulses and incident energy due to the increased pressure gradient. Fig. 11 (a) shows depth of laser-incised holes generally increased with increase in incident energy. A less clear trend was apparent between energy and depth of penetration at 532nm (Fig. 11 (b)). Those points lying outside of the trend are likely influenced by anatomical differences between specimens

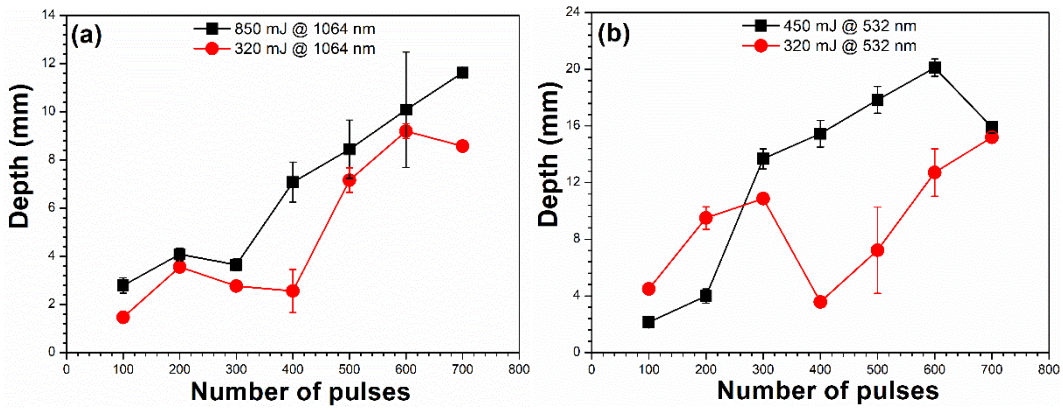


**Fig. 11** Variation of laser-incised hole depth with laser energy at (a) 1064 nm and (b) 532 nm wavelengths in Radiata Pine.

*3.7. Effect of focal point positioning on depth of laser-incised holes*

Fig. 12 shows the effect of focal point positioning on the depth of holes using a laser wavelength of 355 nm which is strongly absorbed by wood. t. The focal point was changed with respect to the surface of the wood (z = 0 mm) to better understand its effect on the laser-incision depth. The focal points were 10 mm (z = +10 mm) above and below (z = -10 mm) the surface. It is evident from Fig. 12 that positioning the focal point away from the surface results in shallower holes due to energy dissipation to the surroundings and hence, less fluence at the surface. A laser beam focused on the surface the wood resulted inhigher incision depth up to 400 laser pulses, beyond which the focal point is positioned below the surface (z = -10 mm) becomes dominant. By analysing the plots relating to z = 0 mm and z = -10 mm, it may be noted that the measured difference in depth of laser-incised holes between 400 pulses and 700 pulses was due to the dominance of the wood anatomy impacting the laser-material interaction, rather than the laser-incision parameters and focal point positioning. Laser irradiation on the latewood tissues resulted in less ablation compared to that seen for the earlywood. Moreover, the laser-incision depth was affected by the presence of earlywood and latewood tissues and their thickness and orientation/inclination with respect to the laser irradiation. The lowest depth of the laser-incised holes for z = -10 mm could also be related to the reduced laser energy density due to the larger spot size on the wood surface.

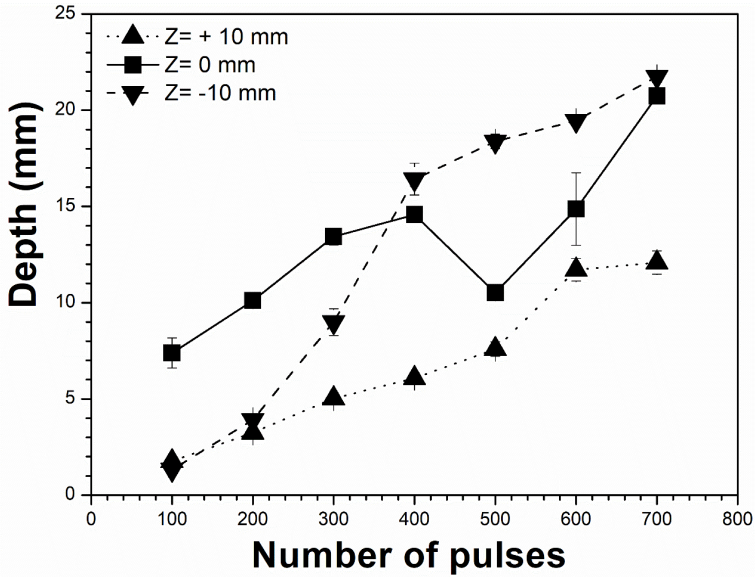


**Fig. 12** Variation in depth of laser-incised holes with laser pulses for a laser wavelength of 355 nm with a laser beam focused above the surface (Z= +10 mm), on the surface (Z= 0 mm) and beneath the surface (Z= -10 mm) of Radiata Pine.

*3.8. Incision rate*

Fig. 13 shows the variation in the depth per pulse (incision rate) with the number of laser pulses (≈ depth) incident on the wood surface for a laser wavelength of 355 nm. From Fig. 13 (a-c), the incision rate varied in a non-monotonic way and is indicated by the change in slopes of the plots. Plotting tangents to the curves revealed a transition point where it is believed that a change in the incision mechanism was taking place. It is evident from Fig. 13 (a) that the incision rate decreased with the number of laser pulses up to 420 beyond which a plateau was observed. The available laser fluence on the surface was believed to be well above the ablation threshold, the laser-incision was fast which slowed down due to decrease in the laser fluence with depth of incision due to laser energy attenuation and a diverging laser beam. The expulsion of vaporised materials was reduced following a gradual decrease in the available laser fluence at the hole front thereby reducing the incision rate with an increase in the number of laser pulses which is evident in Fig. 13 (a). With the focal point positioned 10 mm below the surface, the incision rate increases with the number of laser pulses up to 430 pulses, followed by a gradual decline in the laser-incision rate as shown in Fig. 13 (b). The laser spot size on the surface of the wood was larger for z = -10 mm which resulted in a lower initial incision rate. With the increase in depth of the laser-incised hole, the laser fluence of the converging laser beam increased which accelerated the incision rate. Further increase in the depth of the laser-incised hole, beyond the focal point, led to a decrease in the laser fluence

thereby slowing down the incision rate. On the other hand, with the focal point positioned 10 mm away from the wood surface (Fig. 13 (c)), the incision rate shows the initial decreasing trend up to 400 laser pulses followed by an increasing trend. The diverging laser beam with a larger spot diameter focused on the surface resulted in lower laser fluence, thereby giving rise to a reduced laser-incision rate with the number of pulses. The highly scattered data points in this case may have been affected by the local structure of the wood. Comparing the plots as shown in Fig. 13, the change in the slope of the curves takes place between 400 - 425 laser pulses for all the focal point positioning. The transition point for z= 0 mm represents a depth per pulse of 30 μm, corresponding to the laser pulse number 420. Similarly, the transition points for z= -10 mm and z= + 10 mm represent the depths per pulse of 47 μm and 16 μm, corresponding to the laser pulse numbers of 425 and 400, respectively. Comparing all the focal point positioning, it can be concluded that the depth per pulse for z= -10 mm was the highest at the common transition range (400-425).

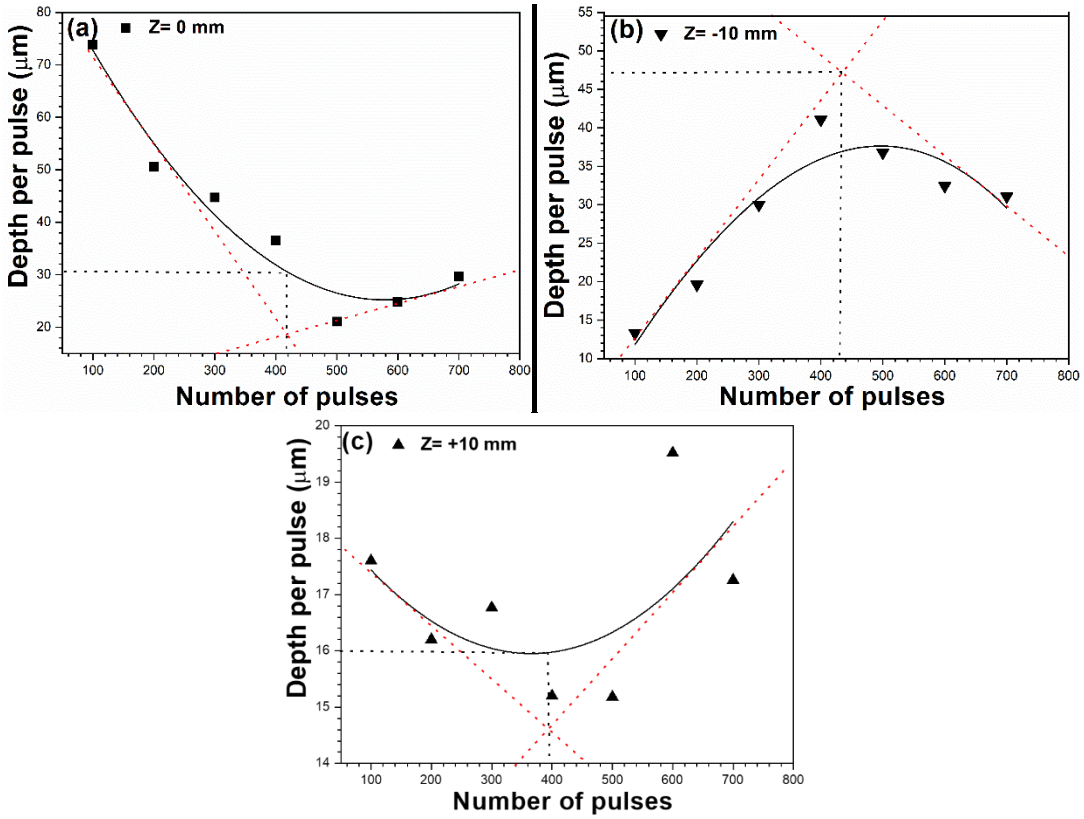


**Fig. 13** Change in depth per pulse with the number of laser pulses for a laser wavelength of 355 nm with a laser beam focused (a) on the surface (Z= 0 mm), (b) beneath the surface (Z= -10 mm) and (c) away from the surface (Z= +10 mm), in Radiata Pine.

## 4. Conclusions

The present investigation focused on establishing settings to produce high aspect ratio holes in Radiata Pine. It was found that laser wavelength, laser energy, pulse number and focus had an influence as did wood anatomy. The influence of laser settings and anatomy on incised hole characteristics were examined. Wood anatomy, notably growth ring orientation relative to the surface and earlywood-latewood ratio had a significant impact on depth and diameter of incised holes under each laser set up. The following conclusions may be drawn;.

1. The laser-incised hole diameter did not show a clear trend with the laser wavelength. A maximum laser-incised hole diameter of ~ 2.5 mm was measured at 1064 nm wavelength for 700 pulses.
2. The shape and size of the laser-incised hole were influenced by growth ring alignment in the wood. The laser interaction with the earlywood and latewood tissues resulted in different laser-incision rates.
3. Significant charring and carbonisation of hole surface and wall were observed at 1064 nm, significantly decreasing with wavelength, with the minimum charring/carbonisation being observed at the 355 nm wavelength.
4. Laser-incised hole taper was more at 1064 nm which decreased with the decrease in the wavelength of the laser.
5. The depth of the laser-incised holes increased with decreasing the wavelength from NIR to UV laser radiation. Maximum depth of the laser-incised hole was measured (~20 mm) for 355 nm wavelength.
6. The laser pulse number also had a significant effect on carbonisation. An increased carbonisation in the hole was observed with higher pulse number. The extent of charring was also seen to be more towards the upper part of the hole.
7. The diameter of laser-incised holes increased with increase in the incident laser energy irrespective of the laser wavelengths. A maximum diameter of ~ 6 mm was measured for the incident laser energy of 850 mJ at 1064 nm wavelength.
8. The depth of laser-incised holes increased with the increase in the laser incident energy.
9. The degree of charring was higher at higher incident laser energy which significantly decreased at lower incident energy.
10. The depth of the laser-incised holes increased with the number of laser pulses for all the studied incident laser energies.

11. Positioning the focal plane away from the surface resulted in a lower depth of incised holes. A laser beam focused on the surface the wood provided better incision performance in terms of higher laser-incision depth up to 400 laser pulses beyond which focal point positioning below the surface becomes dominant.

## 5. Statements and Declarations


### Funding

This work was supported by Innovate UK (LASERCURE: 103545).


### Competing interests

The authors declare no conflict of interests with any individual or organisation in relation to the content of the article.

### Availability of data and material

The authors confirm that all the findings are available in the article itself. More information, if required, may be made available upon request.

### Code availability

Not applicable

### Ethics approval

Not applicable

### Consent to participate

Not applicable

### Consent for publication

All authors consent to the publication of the manuscript.

### Authors' contributions

Subhasisa Nath: Conceptualization, methodology, investigation, formal analysis, writing, visualization; David Waugh: Grant awardee, conceptualization, methodology, review; Graham Ormondroyd: Grant awardee, conceptualization, review; Morwenna Spear: Grant awardee, conceptualization, review; Simon Curling: Review; Andy Pitman: Grant awardee, conceptualization, review; Paul Mason: Grant awardee, conceptualization, review.

### Reference


[1] Sutherland, J.: Revival of structural timber in Britain after 1945. Constr. Hist. 25, 101-113 (2010).

[2] Kohler, J.: Modelling the performance of timber structures - Recent research developments and future challenges. 11th World Conf. Timber Eng. (2010).

[3] Lawrence, A.: Modern timber bridges - An international perspective. Struct. Eng. 86 (18), 26-31 (2008).

[4] Gutkowski, R.M., Williamson, T.G.: Timber bridges: State-of-the-art. J. Struct. Eng. 109(9), 2175-2191 (1983).
[5] Wilkinson, J.G.: Industrial Timber Preservation (1st Edn). Associated Business Press, London (1979).
[6] Eaton, R.A., Hale, M.D.C.: Wood: decay, pests, and protection. Chapman & Hall, New York (1993).
[7] Hill, C.A.S.: Wood Modification: Chemical, Thermal and Other Processes. John Wiley & Sons, New York (2006).
[8] Hansmann, C., Gindl, W., Wimmer, R., Teischinger, A.: Permeability of wood - A review. Drev Vysk Res 47, 1–16 (2002).
[9] Hiziroglu, S.: Basics of Pressure Treatment of Wood. Oklahoma Coop Ext Serv. http://dasnr22.dasnr.okstate.edu/docushare/dsweb/Get/Version-3677/F-5047web.pdf (2004). Accessed 5 May 2021.
[10] Liese, W., Bauch, J.: On anatomical causes of the refractory behaviour of spruce and Douglas fir. Inst Wood Sci 4, 3–14 (1967).
[11] Comstock, G.L.: Directional permeability of softwoods. Wood Fiber 1, 283-89 (1970).
[12] Morris, P.I., Morrell, J.J., Ruddick, J.N.R.: A review of incising as a means of improving treatment of sawnwood. Int Res Gr Wood Modif IRG/WP 94 - 40019 (1994).
[13] Evans, P.D.: The effects of incising on the checking of wood: A review. Int. Wood. Prod. J. 7, 12–25 (2016).
[14] Fukuta, S., Nomura, M., Ikeda, T., Yoshizawa, M., Yamasaki, M., Sasaki, Y.: Wavelength dependence of machining performance in UV-, VIS- and NIR-laser cutting of wood. J Wood Sci 62, 316–323 (2016).
[15] Dahotre, N.B., Harimkar, S.P.: Laser fabrication and machining of materials. 1st Edn Springer, Boston (2008).
[16] Dubey, A.K., Yadava, V.: Laser beam machining-A review. Int. J Mach Tools Manuf 48(6), 609-628 (2008).
[17] Wang, H., Lin, H., Wang, C., Zheng, L., Hu, X.: Laser drilling of structural ceramics—A review. J. Eur. Ceram. Soc. 37, 1157-1173 (2017).
[18] Gautam, G.D., Pandey, A.K.: Pulsed Nd:YAG laser beam drilling: A review. Opt. Laser. Technol. 100, 183-215 (2018).
[19] Zhou, B.H., Mahdavian, S.M.: Experimental and theoretical analyses of cutting nonmetallic materials by low power $CO_2$-laser. J. Mater. Process. Technol. 146(2), 188-192 (2004).
[20] Leone, C., Lopresto, V., De Iorio, I.: Wood engraving by Q-switched diode-pumped frequency-doubled Nd:YAG green laser. Opt. Lasers. Eng. 47(1), 161-168 (2009).
[21] Klimt, B.H.: State of the art in laser marking and engraving. Proc. SPIE 0744, Lasers in motion for industrial applications (1987).
[22] Hattori, N.: Laser processing of wood. Mokuzai Gakkaishi 41, 703–709 (1995).
[23] Fukuta, S., Nomura, M., Ikeda, T., Wakabayashi, K.: Processing characteristics of laser micro incising and possibility of its high speed processing. Eur J Wood Wood Prod 77, 249–255 (2019).
[24] Mazumder, J.: A study of the mechanism of laser cutting of wood. For. Prod. J. 41(10), 53-59(1991).
[25] Nath, S., Waugh, D., Ormondroyd, G., Spear, M., Curling, S., Pitman A., Mason, P.: Laser incising of wood: A Review. Lasers. Eng. 45 (4-6), 381-403 (2020).
[26] Panzner, M., Wiedemann, G., Henneberg, K., Fischer, R., Wittke, T., Dietsch, R.: Experimental investigation of the laser ablation process on wood surfaces. Appl. Surf. Sci. 127-129, 787-792 (1998).
[27] Nath, S., Waugh, D.G., Ormondroyd, G.A., Spear, M.J., Pitman, A.J., Sahoo, S., Curling, S.F., Mason, P.: $CO_2$ laser interactions with wood tissues during single pulse laser-incision. Opt. Laser. Technol. 126, 106069 (2020).
[28] Wang, Y., Ando, K., Hattori, N.: Changes in the anatomy of surface and liquid uptake of wood after laser incising. Wood. Sci. Technol. 47, 447–455 (2013).
[29] Barcikowski, S., Koch, G., Odermatt, J.: Characterisation and modification of the heat affected zone during laser material processing of wood and wood composites. Holz Als Roh - Und Werkst 64, 94–103 (2006).
[30] Islam, M.N., Ando, K., Yamauchi, H., Kobayashi, Y., Hattori, N.: Comparative study between full cell and passive impregnation method of wood preservation for laser-incised Douglas fir lumber. Wood. Sci. Technol. 42, 343–350 (2008).
[31] Hattori, N., Ando, K., Kitayama, S., Nakamura, Y.: Laser incising of wood - Impregnation of columns with water-soluble dye. Mokuzai Gakkaishi 40, 1381–1388 (1994).

[32] Hattori, N., Ida, A., Kitayama, S., Noguchi, M.: Incising wood with a 500 watt Carbon-Dioxide laser. Mokuzai Gakkai-Shi 37, 766–768 (1991).
[33] Nath, S., Waugh, D., Ormondroyd, G., Spear, M., Pitman, A.J., Mason, P.: Laser-incision of wood for the modification of liquid impregnation. Timber 2019, London: IOM3, p. 55–67 (2019).
[34] Spear, M., Pitman, A., Nath, S., Waugh, D., Ormondroyd, G., Mason, P.: Model study to compare drying rate through laser-incisions in beech wood. Timber 2019, London: IOM3, p. 69–78 (2019).
[35] Hattori, N., Matano, T., Okamoto, H., Okamura, K.: Microscopic observations of the solid products deposited on the edge of paper by $CO_2$ laser cutting. Mokuzai Gakkai-Shi 34, 417–422 (1988).
[36] Fukuta, S., Nomura, M., Ikeda, T., Yoshizawa, M., Yamasaki, M., Sasaki, Y.: UV laser machining of wood. Eur. J. Wood. Prod. 74, 261–267 (2016).
[37] Spear, M., Holmberg, J., Nath, S., Pitman, A., Waugh, D., Curling, S., Mason, P., Ormondroyd, G.: Fluid flow in wood: investigation of the influence of laser-incision parameters on uptake and flow paths in four wood species. Timber 2018, London: IOM3, p. 137–144 (2018).
[38] Cramer, S., Kretschmann, D., Lakes, R., Schmidt, T.: Earlywood and latewood elastic properties in loblolly pine. Holzforschung 59, 531-538 (2005).
[39] Kumar, S.: Earlywood-latewood demarcation criteria and their effect on genetic parameters of growth ring density components and efficiency of selection for end-of-rotation density of radiata pine. Silvae Genet 51(5-6), 241-246 (2002).
[40] Naderi, N., Legacéy, S., Chin, S.L.: Preliminary investigations of ultrafast intense laser wood processing. For. Prod. J. 49, 72–76 (1999).
[41] Barnekov, V.G., McMillin, C.W., Huber, H.A. Factors influencing laser cutting of wood. For. Prod. J. 36(1), 55-58 (1986).
[42] Ye, R., Chyan, Y., Zhang, J., Li, Y., Han, X., Kittrell, C., Tour, J.M., Laser-induced graphene formation on wood. Adv. Mater. 29, 1702211-1702217 (2017).
[43] Chyan, Y., Ye, R., Li, Y., Singh, S.P., Arnusch, C.J., Tour, J.M.: Laser-induced graphene by multiple lasing: Toward electronics on cloth, paper, and food. ACS Nano 12, 2176-2183 (2018).
[44] Mahmood, F., Zhang, C., Xie, Y., Stalla, D., Lin, J., Wan, C.: Transforming lignin into porous graphene via direct laser writing for solid-state supercapacitors. RSC Adv 9, 22713-22720 (2019).
[45] Nath, A.K.: Laser drilling of metallic and nonmetallic substrates. In: Hashmi, S., Batalha, G.F., Van Tyne, C.J., Yilbas, B. (ed) Compr. Mater. Process. Elsevier, New York, pp 115-175 (2014).

**List of Tables**



**List of Figures**

**Fig. 4** Schematic representation of the effect of wood structure on laser-incision. (a) laser-incision into earlywood region through radial face and (b) laser-incision into tangential face passes through both earlywood and latewood.

**Fig. 5** Scanning electron micrographs of the cross-section of Nd: YAG laser-incised holes in Radiata Pine at an incident laser energy of 320 mJ incised for 100 pulses with wavelengths of (a, d) 1064 nm, (b, e) 532 nm and (c, f) 355 nm.

**Fig. 6** Scanning electron micrographs of the cross-section of Nd: YAG laser-incised holes in Radiata Pine with a laser wavelength of 355 nm for (a, c) 100 pulses and (b, d) 700 pulses.

**Fig. 7** Variation of laser-incised hole diameter with varying laser wavelength in Radiata Pine.

**Fig. 8** (a) Schematic representation of laser spot size with the laser wavelength, (b) laser-wood interaction map.

**Fig. 9** Variation of laser-incised hole depth with laser wavelength in Radiata Pine.

**Fig. 10** Variation of laser-incised hole diameter with laser energy at (a) 1064 nm and (b) 532 nm wavelengths in Radiata Pine.

**Fig. 11** Variation of laser-incised hole depth with laser energy at (a) 1064 nm and (b) 532 nm wavelengths in Radiata Pine.

**Fig. 12** Variation in depth of laser-incised holes with laser pulses for a laser wavelength of 355 nm with a laser beam focused away from the surface (Z= +10 mm), on the surface (Z= 0 mm) and beneath the surface (Z= -10 mm) in Radiata Pine.

**Fig. 13** Change in depth per pulse with the number of laser pulses for a laser wavelength of 355 nm with a laser beam focused (a) on the surface (Z= 0 mm), (b) beneath the surface (Z= -10 mm) and (c) away from the surface (Z= +10 mm), in Radiata Pine.